

Theoretical study on the nature of band-tail states in amorphous Si

P. A. Fedders

Department of Physics, Washington University, St. Louis, Missouri 63130

D. A. Drabold and S. Nakhmanson

Department of Physics and Astronomy, Ohio University, Athens, Ohio 45701-2979

(Received 10 August 1998)

Band-tail states are routinely invoked in models of *a*-Si:H, including defect pool models and models of light-induced defects. These models describe the band-tail states as being localized on a single stretched bond. However, to our knowledge, there is no theoretical or experimental work to justify these assumptions. In this work we use *ab initio* calculations to support earlier tight-binding calculations that show that the band-tail states are very delocalized—involving large numbers of atoms as the energy is varied from midgap into the tails. Our work also shows that valence-band-tail states are statistically associated with *short* bonds (not long bonds), and conduction-band states with long bonds. We have slightly modified a 512-atom model of *a*-Si due to Djordjevic, Thorpe, and Wooten [Phys. Rev. B **52**, 5688 (1995)] to produce a large model of *a*-Si:H with realistic band tails, radial distribution function, and vibrational spectrum. Above all, we created and used a model with no spectral or geometrical defects. [S0163-1829(98)03148-8]

I. INTRODUCTION

One of the most widely held views of *a*-Si:H is that valence-band-tail states are localized on single stretched bonds, and that these states are intimately connected (through defect pool models) (Ref. 1) with the number of dangling bonds. Further, numerous models of the Staebler-Wronski effect (SWE) of light induced defects² are based on the same picture. To our knowledge there is no experimental or theoretical evidence that these valence-band-tail states are well localized or associated with stretched bonds. In fact, there is some evidence to the contrary. In earlier *ab initio* work, we have shown³ that single or very localized highly strained bonds lead to midgap states and not to band-tail states. More recent work⁴ using tight-binding with supercells of thousands of Si atoms has shown that band tails are very delocalized and range over hundreds of atoms when one reaches well into the tail. This work was performed using orthogonal tight binding for the energy eigenvalues and the cell itself was built by Djordjevic, Thorpe, and Wooten⁵ (DTW), using a (classical) Keating potential.

In this paper we investigate band tailing with *ab initio* calculations of supercells of *a*-Si:H with over 500 atoms and with no topological irregularities leading to a gap state. Although our supercells are considerably smaller than those of Dong and Drabold,⁴ our results generally confirm that work. However, we find that the details of the distribution of sites in the band tails for the hydrogenated supercells differs substantially from the structure in the unhydrogenated supercell models. In the unhydrogenated supercells we find a very definite wandering stringlike structure that is not observed in the hydrogenated supercells. Surprisingly, we also find that average bond lengths weighted by localization yield bond lengths for the valence-band-tail states that are shorter than average, and for the conduction-band-tail states, yield lengths that are longer than average. The DTW cells are created with no geometrical defects, but do contain a few

spectral defects (localized states in the gap) due to badly strained bonds with abnormal bond angles. However, selective removal of Si atoms and hydrogenation removes these spectral defects. Besides the density of states, we also present the pair-correlation functions and phonon density of states for the defect-free supercells. Individual dangling bonds can be treated in these supercells by removing a hydrogen atom.

Supercells formed by many other investigators (using molecular dynamics) suffer from a huge number of defects—often 10–15% or more. We think that it is a *key point* that claiming good agreement with experiment by comparing to one measurement (typically the radial distribution function) while ignoring others is misleading. Models with several percent (or more) concentration of defect states in the optical gap do not represent amorphous Si, and the use of the most impressive Hamiltonian on such a model is inappropriate. Such models are *particularly irrelevant* to studies of band-tail states, since the mixing between the large number of resonant gap states artificially changes the character of the very states whose properties we wish to study.

From the perspective of the “resonant cluster proliferation” model of the Anderson transition (Dong and Drabold),⁴ the periodicity of the supercell compels overlap with “periodic copies” of a localized state in the central cell. It is important to note that the relevant length scale of interactions here is the “size of the localized state” (possibly involving *many* atoms), *not* the interaction range between basis orbitals. Thus, depending on the energy of the tail state, the effect could be small (for compact midgap states) or very large (for states deeper into the tail which occupy a volume comparable to that of the cell).

The traditional scheme of forming a liquid and quenching is not well justified for *a*-Si, since the topology of the liquid is a *predominantly sixfold metal*, topologically remote from *a*-Si. Present simulated quenches are vastly too fast to enable the liquid Si system to find a metastable minimum resem-

bling *a*-Si. This problem is aggravated by the application of first-principles methods, which are much less efficient than classical simulations. It is probably *not* an accident that it is difficult or impossible to make reasonable quality *a*-Si from quenching from the liquid state: even Nature has trouble losing all memory of the topologically completely distinct liquid. In summary, reasonable *uniform* agreement with *all* salient experiments is *essential*.

An additional value of the DTW cells and this extension of their modeling is the large cell size. Obviously cells comparable in volume to or larger than the states they model are essential. Also, strain effects, which are consequences of the periodic boundary conditions (enforcing the artificial supercell periodicity on what is supposed to be a model of a disordered system) are evidently reduced by a larger supercell.

In the remainder of this section we discuss the computational and analytic methodology for this work. In Sec. II we treat the starting point and methodology of creating the supercells as well as their properties. An analysis of the band tails is given in Sec. III, and the results are summarized in Sec. IV.

We used the program of Demkov, Ortega, Sankey, and Grumbach,⁶ “FIREBALL96” to construct and analyze our network. This model generalizes the non-self-consistent local basis Harris functional local-density-approximation scheme of Sankey and co-workers⁷ to an approximate self-consistent form. These local basis density-functional methods have been successful for several other disordered systems: GeSe₂,⁸ *a*-Si,⁹ *a*-GaN,¹⁰ and tetrahedral *a*-C.¹¹

II. SUPERCELL PROPERTIES

A. Ancestral DTW cell

We have found that the well-known work of Wooten and Weaire¹² is still the best starting point for modeling *a*-Si. In this scheme, a simple Keating potential is used to describe interatomic interactions, and four-coordination is constrained (which enables the use of the simple potential). As dangling bonds form a very small fraction of the sites in good-quality *a*-Si, this is not only *reasonable*, but also physically *realistic*.

B. Unhydrogenated relaxed DTW model

To create the first *a*-Si model consistent with a first-principles Hamiltonian involving of order 512 Si atoms and experiment, we simply performed a steepest descent quench of the coordinates provided by DTW, and after some rather minor rearrangements obtained the first structural model employed in this paper. The supercell is denoted by S512H0. The pair-correlation function for this cell is given in Fig. 1. The vibrational spectrum is very similar to that in Fig. 5(a).

For this paper, we focus primarily on the electronic properties. The electronic density of states for S512H0 is shown in Fig. 2, including 15 states above and below the Fermi level. Each bar on the figure represents an energy eigenvalue and the quantity $Q_2(E)$ is a measure of the localization of the state,

$$Q_2(E) = \sum Q(n, E)^2, \quad (1)$$

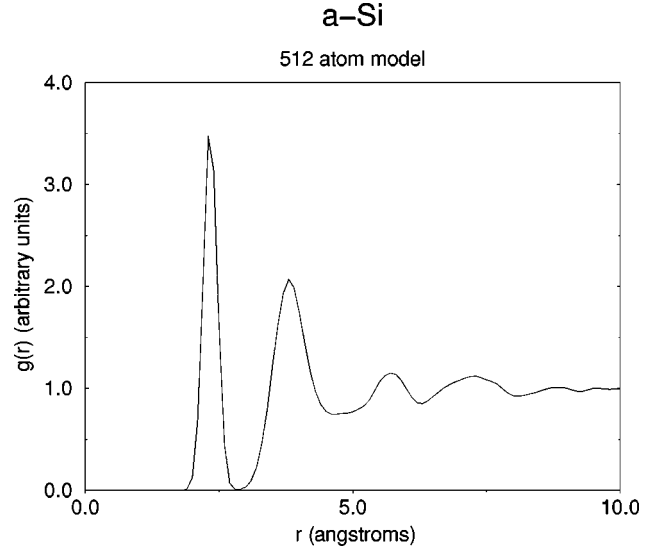


FIG. 1. The pair correlation function for supercell sample S512H0.

where $Q(n, E)$ is the localized charge density associated with the eigenvalue E at the site n . For a perfectly uniform extended state $Q_2(E)$ would be 1, and for a perfectly localized state on only one atom it would be $N = 512$, the number of atoms in the supercell. In an amorphous or glassy substance one does not expect $Q_2(E)$ to be unity for any energy eigenvalue because all states have more weight on some sites than others. This does not mean that the states are “localized” in the sense of charge falling off exponentially in an infinite model; it merely reflects the amorphous nature of the model. In any finite sample it is virtually impossible to define exactly where the band tail ends. In fact, we believe that there is no sharp line between the two in any finite sample. The average value of $Q_2(E)$, averaged over all 2048 energy eigenvalues for the cell under discussion, is 1.9, which is about what one would expect. Further, we have never seen a supercell model using LDA with a $Q_2(E)$ larger than a tenth or two of N . This is in disagreement with Bethe lattice calculations,¹³ which show that $Q_2(E)$ should be about $0.7N$ for an isolated dangling bond. However, we typically find spin polarizations of more than 0.5 on isolated dangling

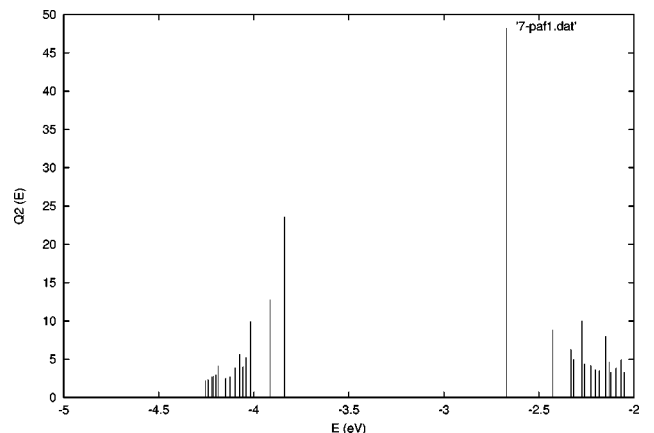


FIG. 2. The electronic density of states for supercell sample S512H0 for the 15 states above and below the gap. The quantity $Q_2(E)$, a measure of localization, is defined in the text.

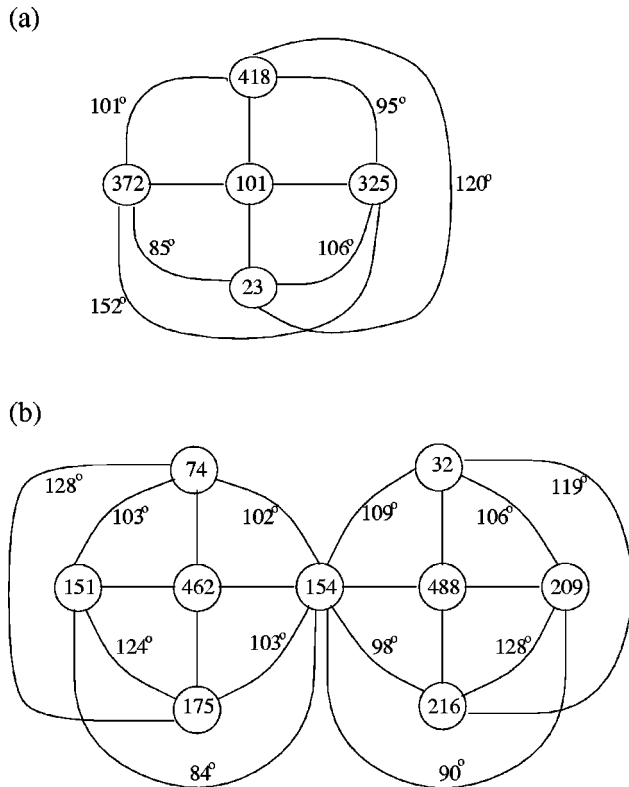


FIG. 3. Depiction of two badly strained regions in supercell sample S512HO. Note the badly strained bond angles.

bonds which is in reasonable agreement with NMR hyperfine studies.¹⁴ See Ref. 15 for a more complete discussion.

In supercell S512H0, we note that the two states in the middle of the gap, just above and just below the Fermi level, are quite localized. This is universal in all unhydrogenated supercells that we have looked at, and is due to badly strained regions of the cell. In the present case Figs. 3(a) and 3(b) depict the two such badly strained regions of the cell. The sketches give two-dimensional representations of the badly distorted bond angles. Only the distorted bond angles are shown. This type of behavior has been seen in numerous supercells of *a*-Si and *a*-C. Such defects are either extremely rare or nonexistent in real *a*-Si, and thus to make a really satisfactory model of *a*-Si they must be removed. This is easily accomplished by extracting the Si atom or atoms at the center of the badly strained region, hydrogenating the dangling bonds, and relaxing or annealing the supercell. We note that if such defects did exist in number of order $10^{14}/\text{cc}$ in real *a*-Si:H, they would have been detected in ESR experiments.

C. Hydrogenated model

It is straightforward to make models of *a*-Si:H starting with a DTW cell while at the same time relieving strain in the network. In particular, one can simply remove atom(s) responsible for deep tail (nearly midgap) states in the H-free model, and hydrogenate the resulting dangling bonds. The NMR proton second moment obtained for such a cluster appears as one component (usually the main one) of the NMR signal.¹⁶ Supercells hydrogenated with the above method yield a NMR broad line in good agreement with

a-Si with Hydrogen

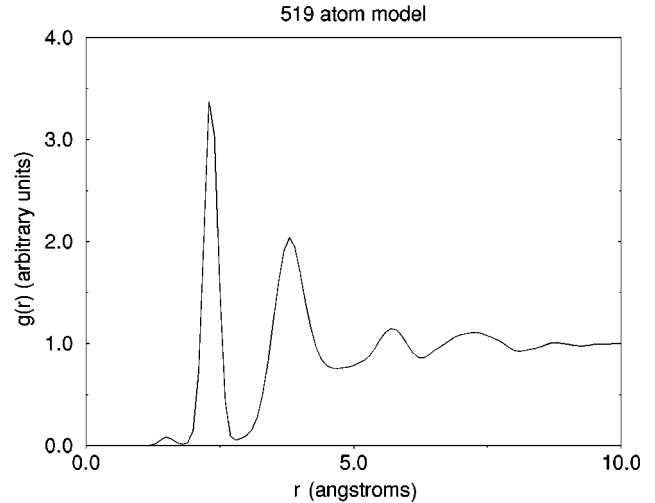


FIG. 4. The pair correlation function for supercell sample S509H10.

experiments.¹⁷ It is of course a limitation of this approach that the H is always clustered, and it cannot be used to create models with isolated (hydrogenated or not) dangling bonds. For the first model with 512 Si atoms and no H atoms, we merely quenched the DTW model since annealing this large a supercell was not feasible.

In detail, to form the hydrogenated model, we removed Si atom 101 and inserted four H atoms to tie up the dangling bonds, and removed the neighboring Si atoms 462 and 154 and inserted six H atoms to tie up the dangling bonds. This supercell model is thus referred to as S509H10. The pair correlation function of the new supercell is given in Fig. 4, and the vibrational spectra in Figs. 5(a) and 5(b). The vibrational spectra agrees well with earlier work in Ref. 3 and with experiments. The density of states is exhibited in Fig. 6. Note the increased gap. The gap is still too small and this is also universally observed in computer-generated supercells. This is true even using orthogonal tight binding with parameters that give an excellent band structure for crystalline Si and a large gap with a Bethe lattice. The reasons are probably the same as discussed in Sec. II B. By removing even more Si atoms and hydrogenating the dangling bonds, the gap can be widened and the localization of the states reduced. However, one needs more and more subtractions to obtain a smaller and smaller improvement.

III. BAND TAILS IN *a*-Si AND *a*-Si:H

A. Background

There are few unambiguous results about band-tail states in amorphous systems. It is usually assumed that band tails (especially valence band tails) originate in single stretched bonds and are thus very localized. This is one of the primary assumptions of the celebrated defect pool model. The other key ingredient is that the total energy of *a*-Si:H is largely determined by the energies of the individual eigenstates. There are significant calculations that dispute both assumptions. The second one was discussed in an earlier paper.¹⁸ This paper concerns the first. Further, dozens of

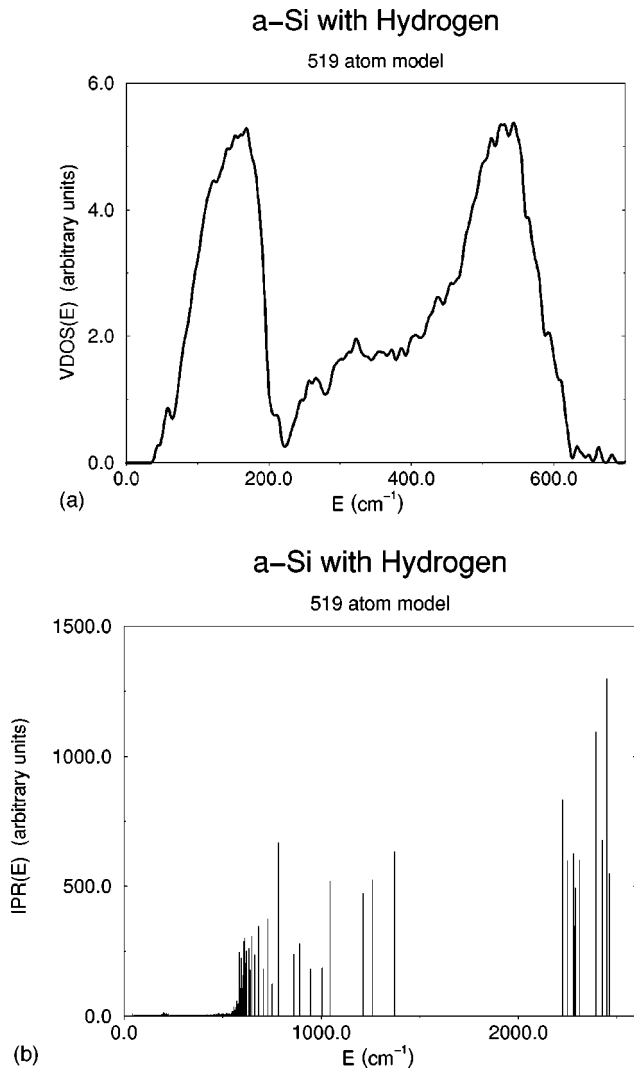


FIG. 5. (a) The vibrational density of states for supercell sample S509H10 in the region of Si modes. (b) The vibrational modes of S509H10 where the inverse participation ratio (IPR) is plotted vs energy.

Staebler-Wronski² models assume that broken strained bonds in the band tails are responsible in one way or another for light-induced defects. This paper offers a significant criticism of this corpus of work, but also complements it and clarifies the microscopic states the defect pool model¹ (DPM) really describes. In particular, the DPM can be interpreted as a very successful phenomenological theory of the Staebler-Wronski effect and recovery from nonequilibrium states. Its success on this type of problem is impressive, and in no way can simulation methods as we present here supplant the fundamental role of the DPM. In the conventional view, DPM describes much of the SWE from a very local picture for the states for which probably inappropriate. However, the DPM is probably equally applicable to the more extended tail states we describe here, and it is interesting to reflect on possible *experimental* indications of the extension of the tail states. The difference between electronic extension and locality in real space should emerge in transport or optical experiments (which are connected to the *lifetimes and overlaps* of various states and associated momentum matrix

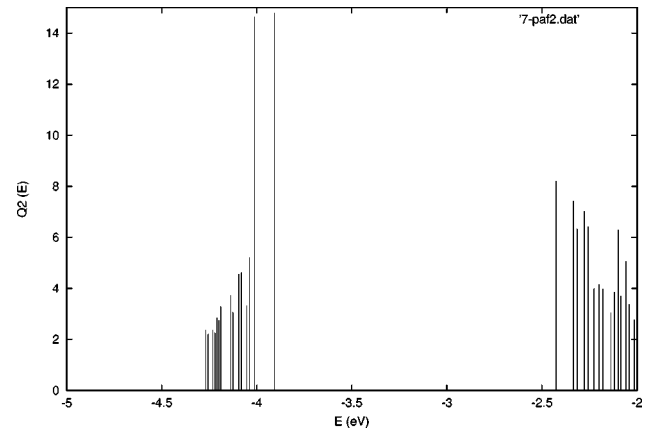


FIG. 6. The electronic density of states for supercell sample S509H10. The quantity $Q_2(E)$ is a measure of localization.

elements), though it may be very difficult to extract such information from current experimental techniques.

Although it is clear that the disordered nature of *a*-Si is responsible for the band tails (especially the *valence*-band tails—the conduction tails are dominated by thermal disorder) there is no quantitative theory of the effect. The reason for this dearth of theory is due to the fact that the effect does not exist in crystalline material (which is much better understood), and also that one needs huge numbers of atoms in a supercell calculation in order to hope to model the effect. This latter follows because the density of band-tail states is at most on the order of tenths of a percent of the number of atoms. Thus one needs tens of thousands of atoms to really treat the problem reasonably. At present, this is not feasible.

In fact, there is quite a bit of theoretical evidence that band-tail states are not very well localized. Several years ago we noticed that the edges of the valence and conduction bands in computer-generated *a*-Si:H were not very well localized at all.³ In fact, the only quasilocalized states caused by strains are states like those caused by the geometrical oddities as depicted in Fig. 3, and these states are roughly midgap, not in the tails. Calculations of band tails on strained Bethe lattices¹⁹ showed that the band tails could be caused by a distribution of strains but this was not a single localized stretched bond. Much more recently Dong and Drabold investigated band tails in a DTW supercell of 4096 Si atoms.⁴ This work showed that the band-tail states were very delocalized except near midgap, and that the localization dropped off rapidly as one went deeper into the band tail. It also made explicit an intuitive view that quantum-mechanical mixing between energetically similar localized “cluster states” was the means by which midgap (Anderson localized) states evolved to extended states (past either mobility edge). The eigenvalues and vectors were calculated only with orthogonal tight binding, and the supercell was not hydrogenated. Of course, one cannot possibly correct these deficiencies and still work with a supercell of thousands of atoms. Further, it would seem extremely unlikely that the delocalization of the band-tail states is due to the above approximations. However, the details could be changed.

B. Results for the new models

First we will consider the average bond length and bond angle associated with band-tail states. In practice, in this con-

TABLE I. Various measures of the average bond length for a numbers of eigenvalues near midgap for supercell S512H0. $L_n(e)$ are defined in the text. Note that the gap is between eigenvalues 1024 and 1025.

e	$L_1(e)$	$L_2(E)$	$L_4(e)$
1009	2.3418	2.3359	2.3266
1011	2.3388	2.3292	2.3153
1013	2.3406	2.3337	2.3265
1015	2.3401	2.3342	2.3234
1017	2.3393	2.3320	2.3270
1019	2.3370	2.3324	2.3249
1021	2.3364	2.3265	2.3150
1023	2.3285	2.3193	2.3183
1024	2.3310	2.3149	2.3002
1025	2.3873	2.4287	2.4682
1026	2.3830	2.4237	2.4699
1028	2.3726	2.3977	2.4242
1030	2.3702	2.3893	2.4128
1032	2.3695	2.3855	2.3944
1034	2.3650	2.3828	2.4022
1036	2.3671	2.3856	2.4096
1038	2.3620	2.3688	2.3772

text, “band-tail states” merely means states near the gap because our supercells are not large enough to identify actual band tails. As noted earlier, a weight or fraction of the charge can be assigned to each atom for a given energy eigenvalue.

To specify an average bond length associated with an energy eigenvalue, e , we define

$$L_n(e) = \frac{\sum [W(e,i)W(e,j)]^n a(i,j)}{\sum [W(e,i)W(e,j)]^n}, \quad (2)$$

where $a(i,j)$ is the bond length between neighboring atoms i and j , $W(e,i)$ is the relative weight of eigenvalue e at site i , and the summation is over all pairs of atoms. Table I is for model S512H0, and the columns are e and L_n , where $n = 1, 2$, and 4 respectively. Table II is the same for the Si-Si bonds for model S509H10, and Table III for the Si-H bonds for S509H10. The weighting details are relatively unimportant. Clearly short Si-Si bonds are associated with v -band states and long Si-Si bonds with c -band states. We believe that the average bond lengths are 2.36 Å in both cases. Further, the Si-H bond does not appear to be correlated with anything.

Now the bond angles. We have tried various types of weightings here and the results appear to be robust. Define

$$A_n(e) = \frac{\sum \theta(i,j,k)[W(e,i) + W(e,j) + W(e,k)]^n}{\sum [W(e,i) + W(e,j) + W(e,k)]^n}, \quad (3)$$

TABLE II. Various measures of the average Si-Si bond length for a number of eigenvalues near midgap for supercell S509H10. $L_n(e)$ are defined in the text. Note that the gap is between eigenvalues 1023 and 1024.

e	$L_1(e)$	$L_2(E)$	$L_4(e)$
1008	2.3390	2.3313	2.3226
1010	2.3413	2.3346	2.3273
1012	2.3404	2.3341	2.3232
1014	2.3393	2.3333	2.3260
1016	2.3367	2.3226	2.3076
1018	2.3348	2.3295	2.3239
1020	2.3352	2.3221	2.3135
1022	2.3198	2.2958	2.2806
1023	2.3277	2.3197	2.3197
1024	2.3815	2.4200	2.4641
1025	2.3576	2.3617	2.3736
1027	2.3649	2.3774	2.3985
1029	2.3658	2.3826	2.4036
1031	2.3590	2.3680	2.3853
1033	2.3695	2.3921	2.4159
1035	2.3673	2.3847	2.4049
1037	2.3608	2.3779	2.4021

$$B_n(e) = \frac{\sum \theta(i,j,k)[W(e,i)W(e,j)W(e,k)]^n}{\sum [W(e,i)W(e,j)W(e,k)]^n}, \quad (4)$$

where weighting $W(e,i)$ is the same as before, $\theta(i,j,k)$ is the angle formed by the atoms i - j - k measured in degrees and with 109.47° subtracted from it. In Tables IV, V, and VI the columns are e , A_1 , A_2 , B_1 , and B_2 , respectively. Table

TABLE III. Various measures of the average Si-H bond length for a number of eigenvalues near midgap for supercell S509H10. $L_n(e)$ are defined in the text. Note that the gap is between eigenvalues 1023 and 1024.

e	$L_1(e)$	$L_2(E)$	$L_4(e)$
1008	1.5286	1.5289	1.5296
1010	1.5238	1.5245	1.5277
1012	1.5259	1.5236	1.5219
1014	1.5270	1.5268	1.5253
1016	1.5243	1.5224	1.5220
1018	1.5236	1.5221	1.5221
1020	1.5274	1.5257	1.5233
1022	1.5342	1.5407	1.5427
1023	1.5228	1.5177	1.5156
1024	1.5237	1.5213	1.5211
1025	1.5253	1.5235	1.5216
1027	1.5254	1.5227	1.5206
1029	1.5320	1.5343	1.5367
1031	1.5243	1.5214	1.5194
1033	1.5306	1.5317	1.5336
1035	1.5291	1.5287	1.5277
1037	1.5255	1.5230	1.5180

TABLE IV. Various measures of the average bond angle for a number of eigenvalues near midgap for supercell S512H0. A_n and B_n are defined in the text.

e	$A_1(e)$	$A_2(E)$	$B_1(e)$	$B_2(e)$
1009	10.45	10.73	10.89	10.90
1011	10.58	11.12	11.66	10.96
1013	10.51	11.02	11.66	12.11
1015	10.68	11.45	13.44	15.90
1017	10.68	11.20	11.82	12.82
1019	10.93	11.71	12.91	13.92
1021	10.52	10.93	11.84	13.63
1023	11.33	12.85	14.16	13.92
1024	11.83	13.22	16.20	16.15
1025	12.42	16.35	29.03	37.80
1026	10.15	9.75	9.39	8.27
1028	10.33	10.33	13.38	16.26
1030	10.50	11.30	13.38	16.26
1032	10.33	11.10	12.58	13.83
1034	10.27	11.62	14.82	18.93
1036	10.44	10.93	12.20	12.93
1038	10.80	12.85	17.18	21.11

IV is for model S512H0, Table V is for model S509H10 for triads containing no H, and Table VI for S509H10 with triads containing one H atom. Interestingly enough, hydrogenation has very little effect on the average bond lengths, and the Si-H bond lengths do not correlate in the same way that Si-Si bond lengths do. However, as we shall see, H has a large effect of the topology of the strained bonds.

These results are rather startling, at least to us. Thus we have checked the results in a couple of different ways. First we calculated the same averages for a model of 71 atoms (61 Si and ten H) that was created in an entirely different way,

TABLE V. Various measures of the average bond angle for triads not involving H's for supercell S509H0. A_n and B_n are defined in the text.

e	$A_1(e)$	$A_2(E)$	$B_1(e)$	$B_2(e)$
1008	10.43	11.05	12.09	14.51
1010	10.50	11.20	12.20	13.72
1012	10.58	11.10	11.60	10.85
1014	10.46	10.85	11.46	12.47
1016	10.84	11.83	12.38	12.73
1018	10.49	11.29	13.82	17.28
1020	10.90	11.81	13.13	14.07
1022	10.43	10.41	11.10	11.38
1023	11.45	13.15	14.49	14.15
1024	10.13	9.79	9.48	8.27
1025	10.82	12.38	14.96	17.42
1027	10.44	11.19	12.71	14.49
1029	10.48	11.37	12.67	14.49
1031	10.66	11.84	14.27	16.37
1033	10.46	10.99	11.61	10.75
1035	10.12	10.56	13.09	18.27
1037	10.39	10.93	12.17	12.51

TABLE VI. Various measures of the average bond angle for triads containing one H for supercell S509H10. A_n and B_n are defined in the text.

e	$A_1(e)$	$A_2(E)$	$B_1(e)$	$B_2(e)$
1008	6.73	8.01	33.60	5.50
1010	7.82	9.08	11.32	6.38
1012	7.09	9.11	41.56	9.62
1014	7.47	8.36	27.37	3.94
1016	7.24	7.18	11.36	5.77
1018	5.65	5.76	16.22	5.63
1020	7.00	7.97	17.65	5.50
1022	5.66	4.77	53.46	4.64
1023	7.26	10.68	11.16	12.56
1024	9.94	10.58	16.14	9.42
1025	9.15	11.03	20.69	9.48
1027	8.42	12.23	18.00	18.47
1029	6.97	10.34	49.62	8.64
1031	7.97	10.73	24.60	12.04
1033	8.44	11.14	42.37	6.24
1035	6.35	6.70	21.23	2.76
1037	7.20	7.03	17.67	3.73

thoroughly annealed, and shown to be absolutely stable at reasonable temperatures. The results were qualitatively the same and different in detail only slightly. That is, the magnitude and trends were identical with only the statistical fluctuations differing. Thus we believe the results to be independent of supercell model as long as one has relaxed the supercell with a good *ab initio* code.

Finally we consider the topology and localization of the strained bonds. As far as the localization vs position in the gap, we can only say that our results are consistent with the earlier study,⁴ and those results are much more detailed because the supercell was much larger. However, we find that the topology of the strained bonds is greatly affected by hydrogenation. These results are rather hard to present, so we resort to crude maps of sketches of the topology of the sites that are most localized for each eigenvalue. These are given by Figs. 7 for the unhydrogenated supercell model S512H0. In each figure all atoms are included with values of $Q(e, n)$ greater than the stated amount, and the bond lengths are noted. One can see that the sites where the state is most localized (and the shortest bonds) for a sort of string or random walk as noted earlier. All or almost all of the sites with the largest weighting are nearest neighbors. This structure was also found by Dong and Drabold.

This effect is absent for the hydrogenated model S509H10. In fact, for the states nearest at the gap, there was at most one pair per state that were nearest or next-nearest neighbors. Thus, the topology of the band-tail states and strains are profoundly altered by the addition of H.

IV. DISCUSSION AND CONCLUSION

The extension of the band tails observed here and elsewhere is a point of some importance, and we emphasize that it should strongly affect DPM's, and the modeling of transport in amorphous Si. We have also detected some statistical

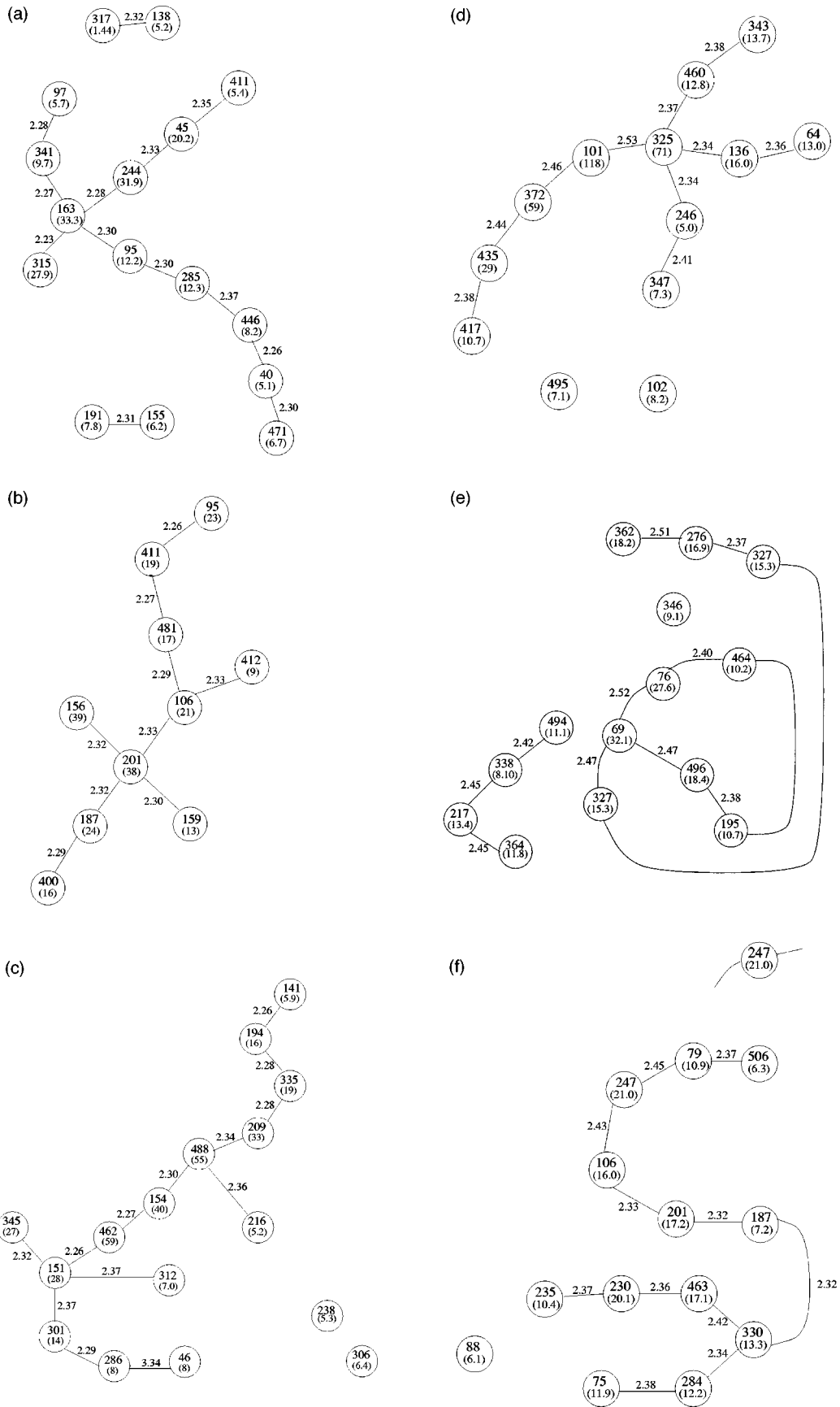


FIG. 7. Crude topological maps for sites at which the charge is most localized for a number of eigenvalues near the Fermi surface. Parts (a)–(f) refer to eigenvalues 1022–1027, respectively, and the gap is between eigenvalues 1024 and 1025. The circles represent the atoms where the atom number and value of Q_2 (in parentheses) are given. The bond lengths in Å are given on the bonds. Circles not connected by bonds to other circles are not nearest neighbors to any of the other sites in the diagram.

correlations between bond lengths and energy eigenvalues; the valence tails being associated with short bonds and the conduction tails with long bonds. In some sense the conduction-band result can easily be “explained.” As atoms are pushed further apart, the conduction band will drop since it is made of antibonding states. However, then one might expect the valence band to drop as the atoms grow closer together, and this is not observed. The answer lies along different directions. If one takes a crystal and distorts it slightly, both the conduction and valence bands will tend to move toward the center of the gap. The reason is simply that symmetries are broken and degenerate states split. To first order, the center of gravity of the split does not move as some states move up and some move down. Thus the gap will tend to close up. The same effect holds with *a*-Si—at least with the Bethe lattice. With a perfect Bethe lattice, any local perturbations in bond length or bond angle will tend to move the conduction band down and the valence band up. We believe that an analog of this is happening in our model. However, we would have expected more of a bond-angle effect than a bond-length effect. We must be careful to distinguish two things being correlated from with one thing causing another. Here the bond lengths and band tails are correlated but not necessarily causally.

The defect pool model is usually derived (or justified) on rather detailed kinetic arguments, and/or rather detailed mod-

els on the formation of dangling bond defects from the band tail. We believe that our work casts an enormous amount of doubt on the theoretical underpinning of these models. However, that is not to say that we believe that the defect pool is nonsense. In fact, one does not need the detailed models alluded to above in order to obtain the defect pool model. Basic laws can be assumed much as the rule for tight binding can be assumed. While orthogonal tight binding is based on the unphysical assumptions that orthogonality, overlap, and lack of three-center terms are wrong, tight binding works quite well for some things, especially things that are close to situations that the fitting parameters came from. We view the defect pool model to be in a similar situation.

Note added in proof. We recently performed calculations on models of *a*-Si:H in the local spin density approximation (LSDA) and find that an isolated dangling-bond wave function is as well localized as in spin resonance experiments. Thus LSDA seems to be necessary for describing an unpaired, isolated spin at the Fermi level. However, this is not relevant to band-tail states.

ACKNOWLEDGMENTS

D.A.D. acknowledges the support of the NSF under Grant No. DMR 96-18789. We thank Dr. Jianjun Dong for many helpful discussions.

-
- ¹See, for example, R. A. Street, *Phys. Rev. B* **43**, 2454 (1991); R. A. Street and K. Winer, *ibid.* **40**, 6236 (1989); M. J. Powell and S. C. Deane, *ibid.* **48**, 10 815 (1993); P. C. Taylor, in *Hydrogenated Amorphous Silicon, Part C: Electronic and Transport Properties*, edited by J. I. Pankove, Semiconductors and Semimetals Vol. 21 (Academic, Orlando, FL, 1984), p. 99, and references therein.
- ²There is a vast number of models and references on this subject. For a recent summary see H. Fritzsche, in *Amorphous and Microcrystalline Silicon Technology—1997*, edited by Sigurd Wagner, Michael Hack, Eric A. Schiff, Ruud Schropp, and Isamu Shimizu, MRS Symposia Proceedings No. 467 (Materials Research Society, Pittsburgh, 1997), p. 19, and references therein.
- ³P. A. Fedders, D. A. Drabold, and Stefan Klemm, *Phys. Rev. B* **45**, 4048 (1992); P. A. Fedders and D. A. Drabold, *ibid.* **47**, 13 277 (1993).
- ⁴Jianjun Dong and D. A. Drabold, *Phys. Rev. Lett.* **80**, 1928 (1998).
- ⁵B. R. Djordjevic, M. F. Thorpe, and F. Wooten, *Phys. Rev. B* **52**, 5685 (1995).
- ⁶A. A. Demkov, J. Ortega, O. F. Sankey, and M. P. Grumbach, *Phys. Rev. B* **52**, 1618 (1995).
- ⁷O. F. Sankey and D. J. Niklewski, *Phys. Rev. B* **40**, 3979 (1989); O. F. Sankey and D. A. Drabold, *Bull. Am. Phys. Soc.* **36**, 924 (1991).
- ⁸M. Cobb and D. A. Drabold, *Phys. Rev. B* **56**, 3054 (1997).
- ⁹P. A. Fedders and D. A. Drabold, *Phys. Rev. B* **56**, 1864 (1997).
- ¹⁰P. Stumm and D. A. Drabold, *Phys. Rev. Lett.* **79**, 677 (1997).
- ¹¹D. A. Drabold, P. A. Fedders, and P. Stumm, *Phys. Rev. B* **49**, 16 415 (1994).
- ¹²F. Wooten and D. Weaire, in *Solid State Physics*, edited by H. Ehrenreich and D. Turnbull (Academic, New York, 1984). Vol. 40, p. 2.
- ¹³D. K. Biegelsen and M. Stutzmann, *Phys. Rev. B* **33**, 3006 (1986).
- ¹⁴P. A. Fedders and A. E. Carlsson, *Phys. Rev. B* **37**, 8506 (1988); **39**, 1134 (1989) (0.7 paper).
- ¹⁵S. Estreicher and P. A. Fedders, in *Computational Studies of New Materials*, edited by D. A. Jelsh and T. F. George (World Scientific, Singapore, 1998).
- ¹⁶Karen Gleason, Mark Petrich, and Jeffrey A. Reimer, *Phys. Rev. B* **36**, 3259 (1987).
- ¹⁷P. A. Fedders and D. A. Drabold, *Phys. Rev. B* **47**, 13 277 (1993).
- ¹⁸D. A. Drabold, P. A. Fedders, Stefan Klemm, and O. F. Sankey, *Phys. Rev. Lett.* **67**, 2179 (1991).
- ¹⁹Brian N. Davidson, Ph.D. thesis, North Carolina State University, 1992.